

# **t-kuarkın Anormal Etkileşmelerinin TeV Enerjili Çarpıştırıcılarda Aranması**

İlkay TÜRK ÇAKIR  
Giresun Üniversitesi

Maddenin Yeni Yapı Düzeyi: PREONLAR Çalıştayı, TOBB ETU, 8-10 Mart 2018



# Searches for FCNC $tq\gamma$ Couplings

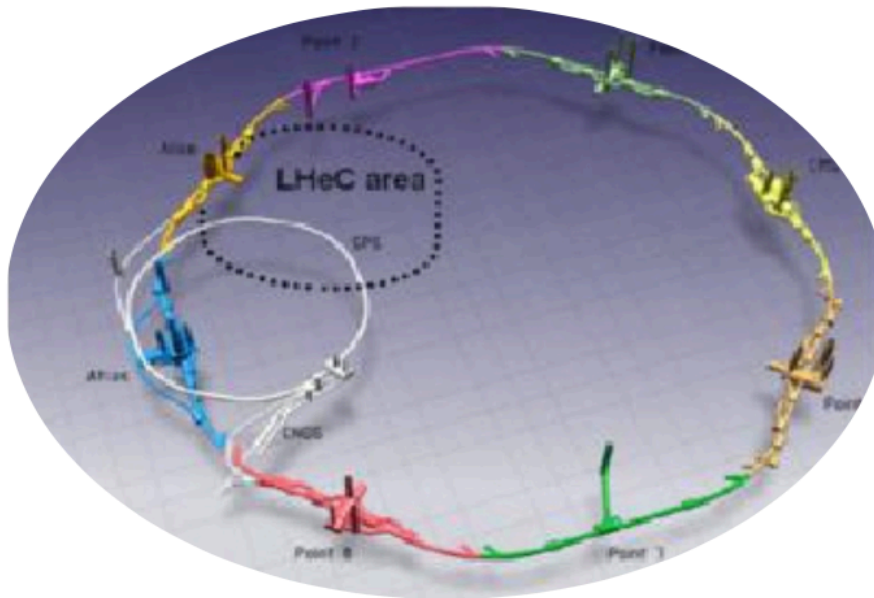
**İlkay TÜRK ÇAKIR**

**with collaboration**

**A. Yılmaz, A. Şenol, H. Karadeniz, O. Çakır, H. Denizli**

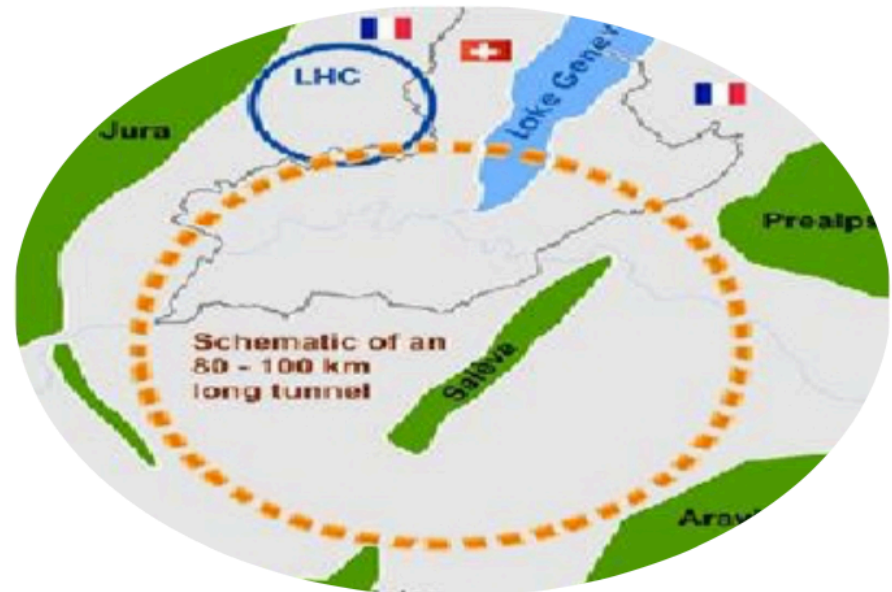
# FUTURE PROSPECTS OF EP COLLIDERS

---



## LHeC

7 TeV proton of LHC  
and 60 GeV electron  
( $\sqrt{s} \sim 1.3$  TeV)



## FCC-he

50 TeV proton of FCC  
and 60 GeV electron  
( $\sqrt{s} \sim 3.5$  TeV)



The top quark FCNC ( $tq\gamma$ ) interactions are described by an effective Lagrangian

$$L_{eff} = \frac{g_e}{2m_t} \bar{t} \sigma^{\mu\nu} (\lambda_u^L P_L + \lambda_u^R P_R) u A_{\mu\nu} + \frac{g_e}{2m_t} \bar{t} \sigma^{\mu\nu} (\lambda_c^L P_L + \lambda_c^R P_R) c A_{\mu\nu} + h.c.$$

LH  
coupling

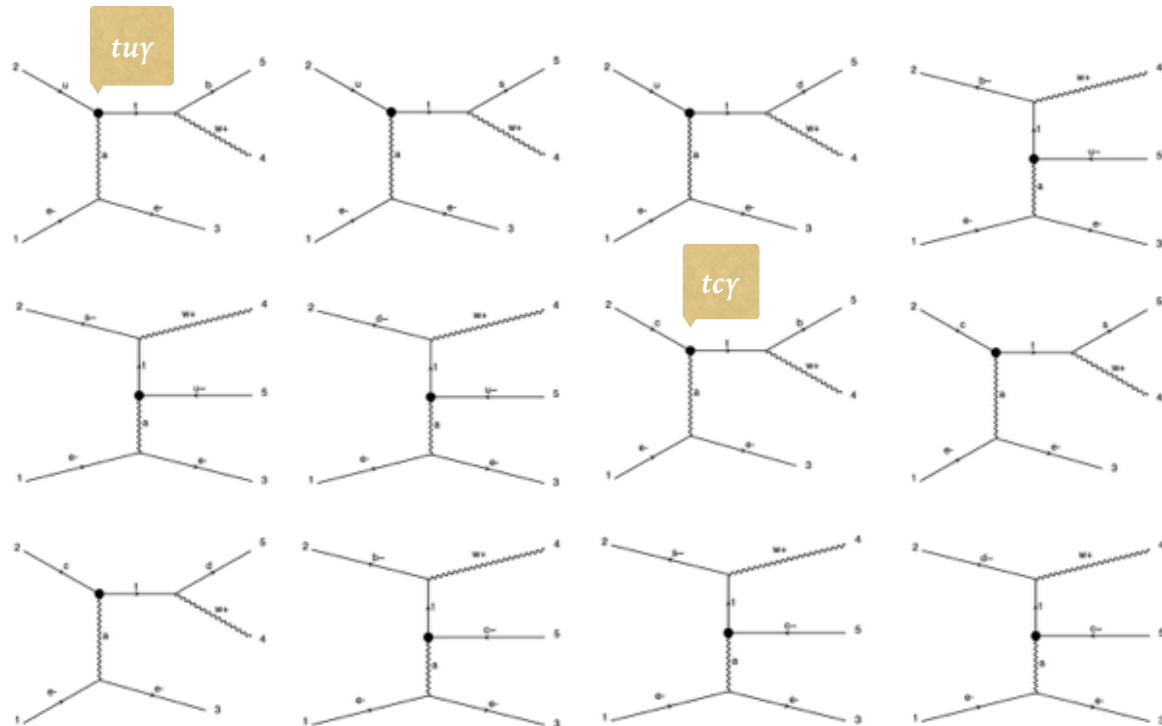
RH  
coupling

LH  
coupling

RH  
coupling

In this study, no specific chirality is assumed for FCNC  $tq\gamma$ , then we take  $\lambda_q^L = \lambda_q^R = \lambda_q$ . Production process is  $e^- p \rightarrow e^- W q + X$ .

There are also similar diagrams for process  $e^- p \rightarrow e^- W^- q + X$  with the interchange  $q \leftrightarrow \bar{q}$ .



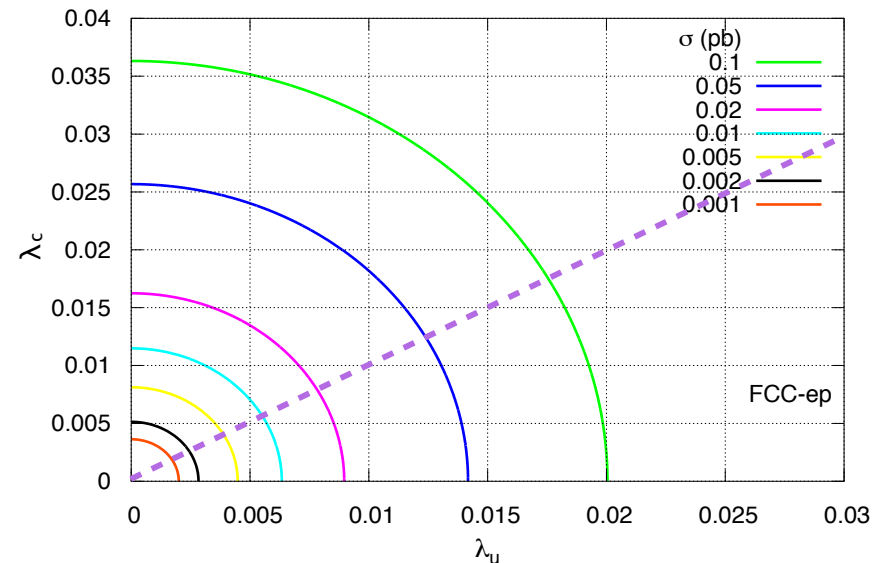
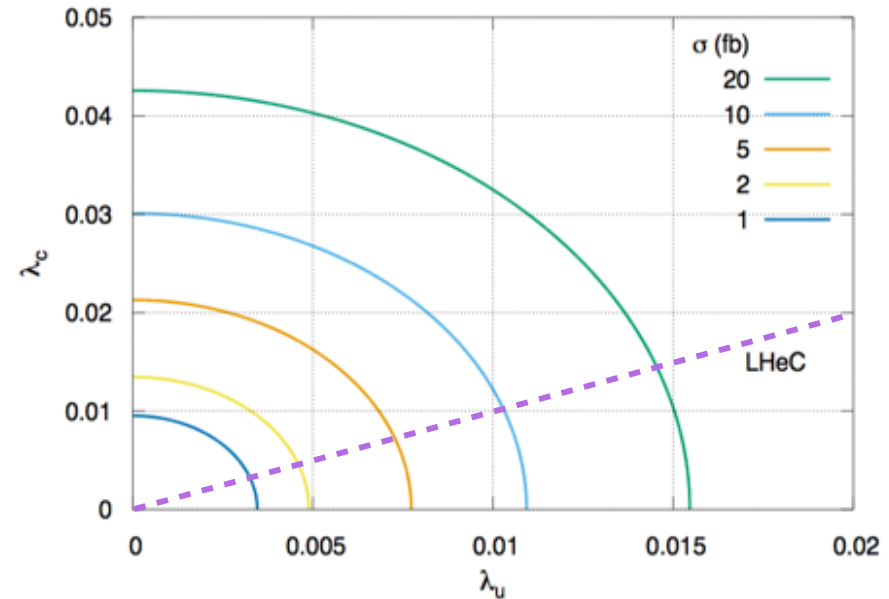


## Process: $e^-p \rightarrow e^-Wq+X$

A contour plot for top FCNC tqy couplings  $\lambda_u$  and  $\lambda_c$  within the interested range depending on different signal cross sections at LHeC collider.

A similar plot depending on the cross section values at FCC-eh. The dashed line corresponds to equal coupling values ( $\lambda_u = \lambda_c$ ) and the sensitivity to  $\lambda_c$  are more pronounced at FCC-eh.

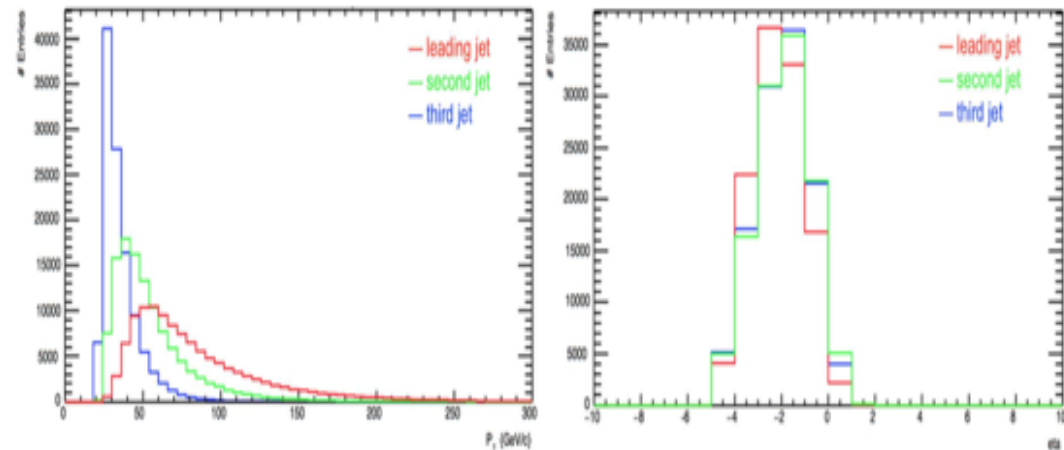
In order to reach a target value of  $\lambda_u=0.01$ , corresponding signal cross section values can be predicted as 8 fb at LHeC and 25 fb at FCC-eh.



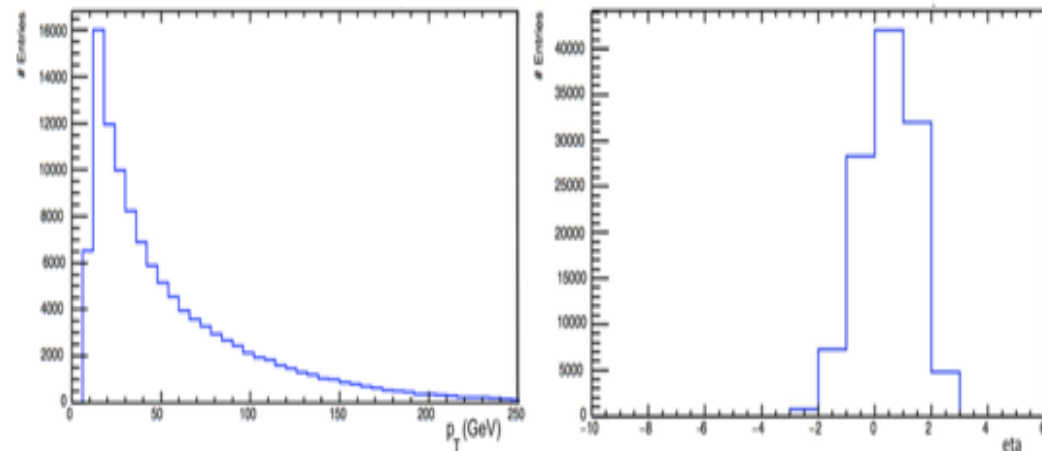
## Kinematical distributions

LHeC

Transverse momentum and pseudo-rapidity distributions of three jets from the process  $e-p \rightarrow e-W^\pm q+X$  which includes both the interfering background and signal for  $\lambda_u=\lambda_c=0.05$  at the LHeC.



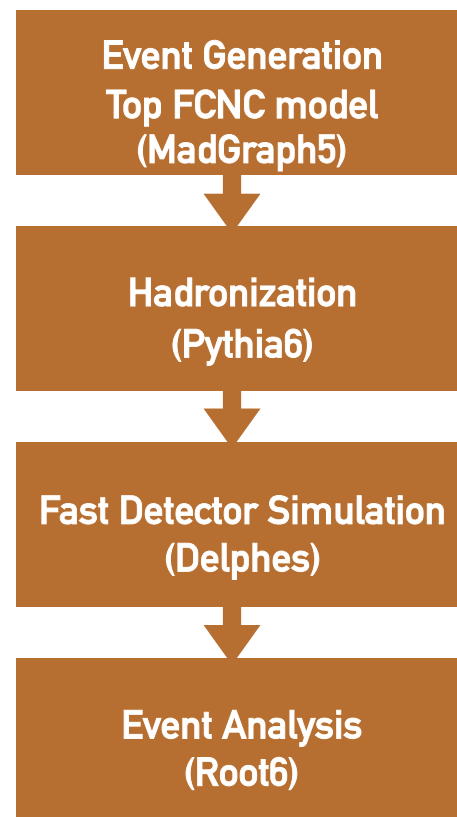
Transverse momentum and pseudo-rapidity distribution of electron for the process  $e-p \rightarrow e-W^\pm q+X$  which includes  $S+B_W$ .



## Analysis

For the analysis, after pre-selection cuts, we use the analysis cuts for further background suppression.

### cut flow

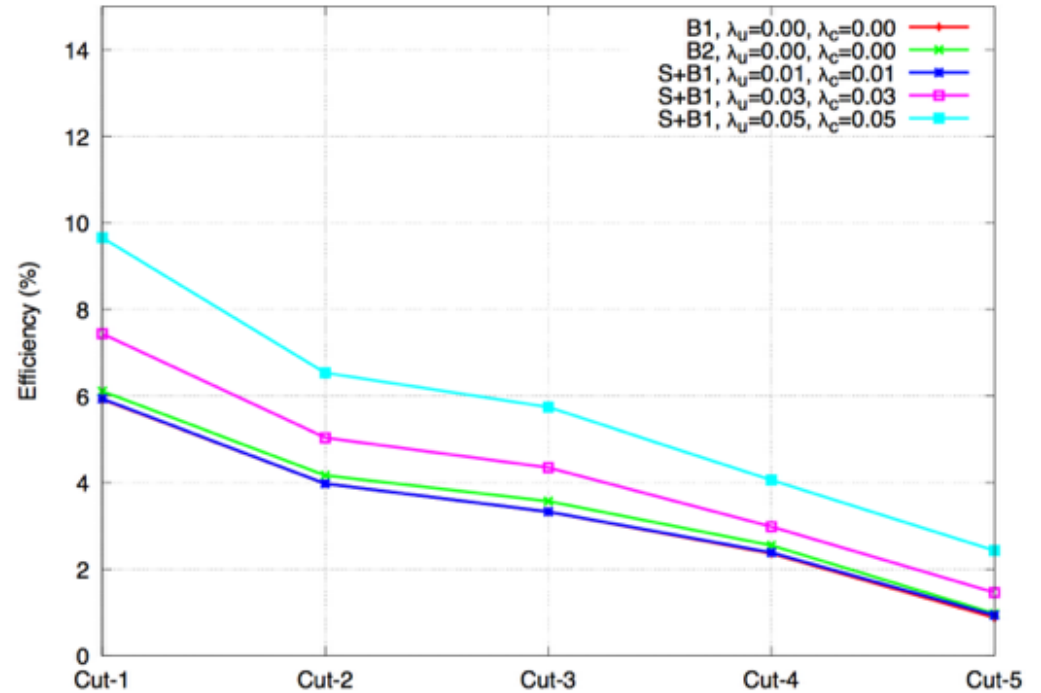


|         |   |
|---------|---|
| Cut-0 : | at least one electron and three jets (pre-selection with default MG5 cuts)  |
| Cut-1 : | require one of three jets as being b-tag  |
| Cut-2 : | b-tagged jet has transverse momentum $p_T > 35$ GeV and other jets have $p_T > 25$ GeV, and electron has $p_T > 20$ GeV |
| Cut-3 : | all jets have pseudo-rapidity $-5.0 < \eta < 0$ ; and electron has $-2.5 < \eta < 2.5$                                  |
| Cut-4 : | invariant mass of two jets within $50 < m_{jj} < 90$ GeV (for W- boson)   |
| Cut-5 : | invariant mass of three jets (for top) between $130 < m_{bjj} < 200$ GeV  |

LHeC

## Cut efficiency

Efficiency plot for the cuts applied at each step for the analysis of signal (S) +background B1(eWq) and eZq(B2) events. The cut efficiencies are calculated with respect to the preselection cuts for each coupling value.



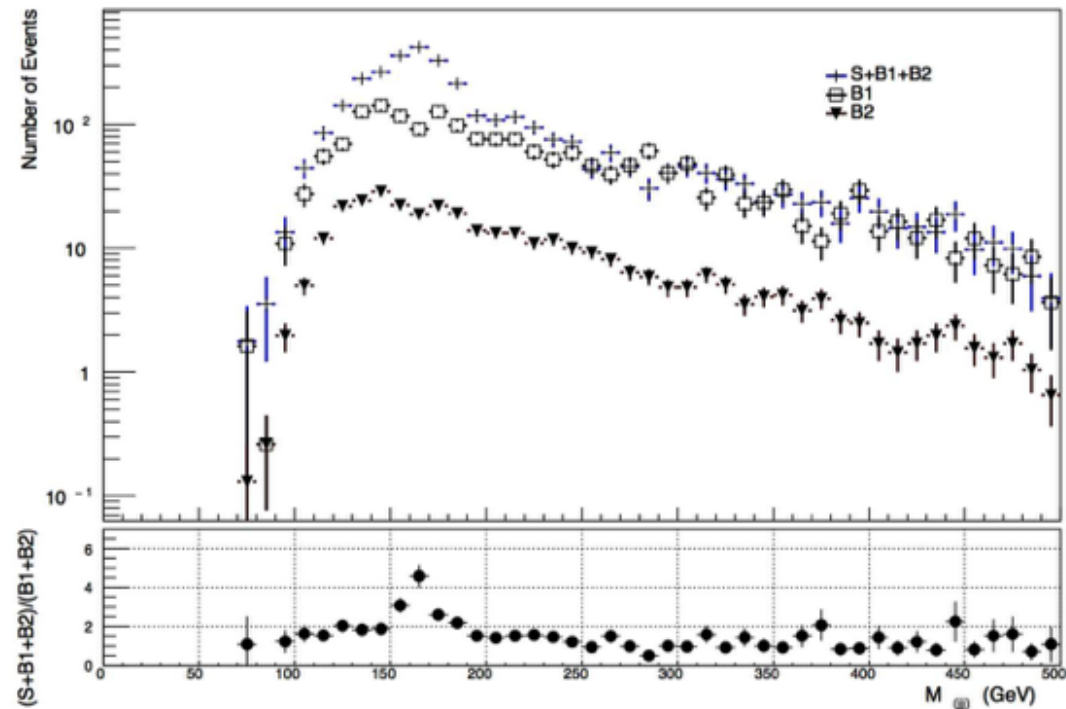
The number of events (N) for background B1 (B2), and signal for different values of  $\lambda_u$  and  $\lambda_c$  at LHeC with  $L_{\text{int}} = 100 \text{ fb}^{-1}$ .

| N                  | $\lambda_c = 0$ | $\lambda_c = 0.01$ | $\lambda_c = 0.03$ | $\lambda_c = 0.05$ |
|--------------------|-----------------|--------------------|--------------------|--------------------|
| $\lambda_u = 0$    | 584 (149)       | 592                | 609                | 640                |
| $\lambda_u = 0.01$ | 617             | 621                | 692                | 763                |
| $\lambda_u = 0.03$ | 943             | 969                | 1003               | 1209               |
| $\lambda_u = 0.05$ | 1502            | 1744               | 1758               | 1792               |

## Invariant mass distributions

LHeC

Invariant mass distributions of three jets (one of the jets is required as b-jet) for the signal +background (S+B1+B2), and backgrounds (B1, B2). The ratio plot presents the signal (for equal coupling scenario  $\lambda=0.05$ ) strength which peaks at the top mass.



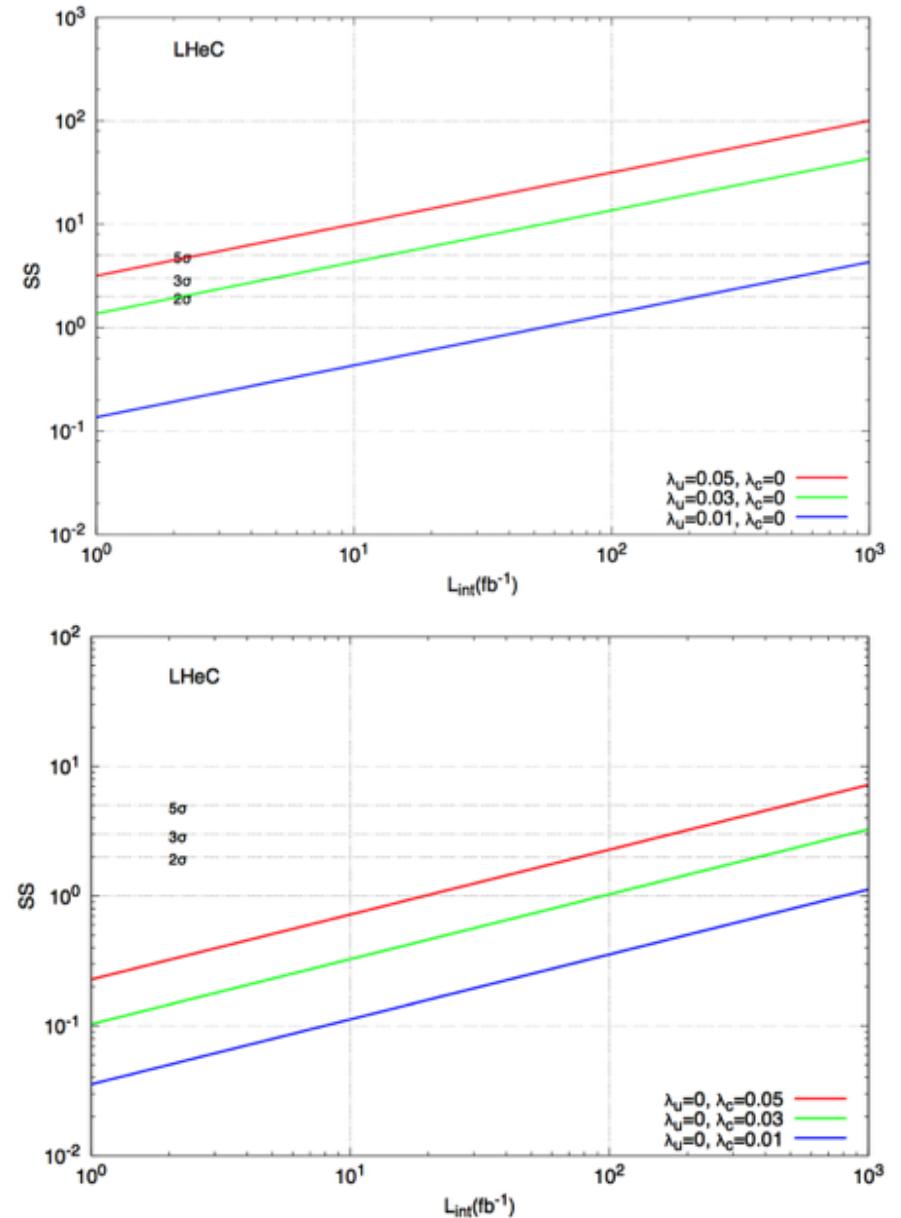
The statistical significance (SS) are calculated at the final stage of the cuts using the signal (S) and total background (B) events.

$$SS = \sqrt{2[(S + B) \ln(1 + \frac{S}{B}) - S]}$$

## Statistical significance

Estimated statistical significance (SS) reach of flavor changing neutral current **tu $\gamma$  coupling** ( $\lambda_u$ ) depending on the integrated luminosity ranging from  $1 \text{ fb}^{-1}$  to  $1 \text{ ab}^{-1}$  at the LHeC. It includes the contribution from the main backgrounds on the results. The signal significance corresponding to  $2\sigma$ ,  $3\sigma$  and  $5\sigma$  lines are also shown.

The SS reach for the flavor changing neutral current **tc $\gamma$  coupling** ( $\lambda_c$ ) depending on the integrated luminosity at the LHeC.



## Analysis of the signal and background at FCC-eh

**Studied processes:**  $e^-p \rightarrow e^-Wq+X$  and  $e^-p \rightarrow e^-Wbq+X$

The event selection and cuts on kinematic variables are applied similarly. Our signal processes include on-shell  $W$  boson and it decays into two jets, therefore we classified the background according to  $e+V+jets$  which includes  $eWj$  ( $B_W$ ) and  $eZj$  ( $B_Z$ ), and we also consider the backgrounds  $eHj$  ( $B_H$ ),  $e\bar{t}t$  ( $B_{tt}$ ) and  $ebjj$  ( $B_{bjj}$ ) backgrounds.

- The signal cross sections (pb) are shown in the following tables

$e^-p \rightarrow e^-Wb+X$

| FCC-he                | $\lambda_c = 10^{-2}$  | $\lambda_c = 10^{-3}$  | $\lambda_c = 0$        |
|-----------------------|------------------------|------------------------|------------------------|
| $\lambda_u = 10^{-2}$ | $3.238 \times 10^{-2}$ | $2.490 \times 10^{-2}$ | $2.488 \times 10^{-2}$ |
| $\lambda_u = 10^{-3}$ | $7.834 \times 10^{-3}$ | $3.243 \times 10^{-4}$ | $2.480 \times 10^{-4}$ |
| $\lambda_u = 0$       | $7.576 \times 10^{-3}$ | $7.580 \times 10^{-5}$ | 0                      |

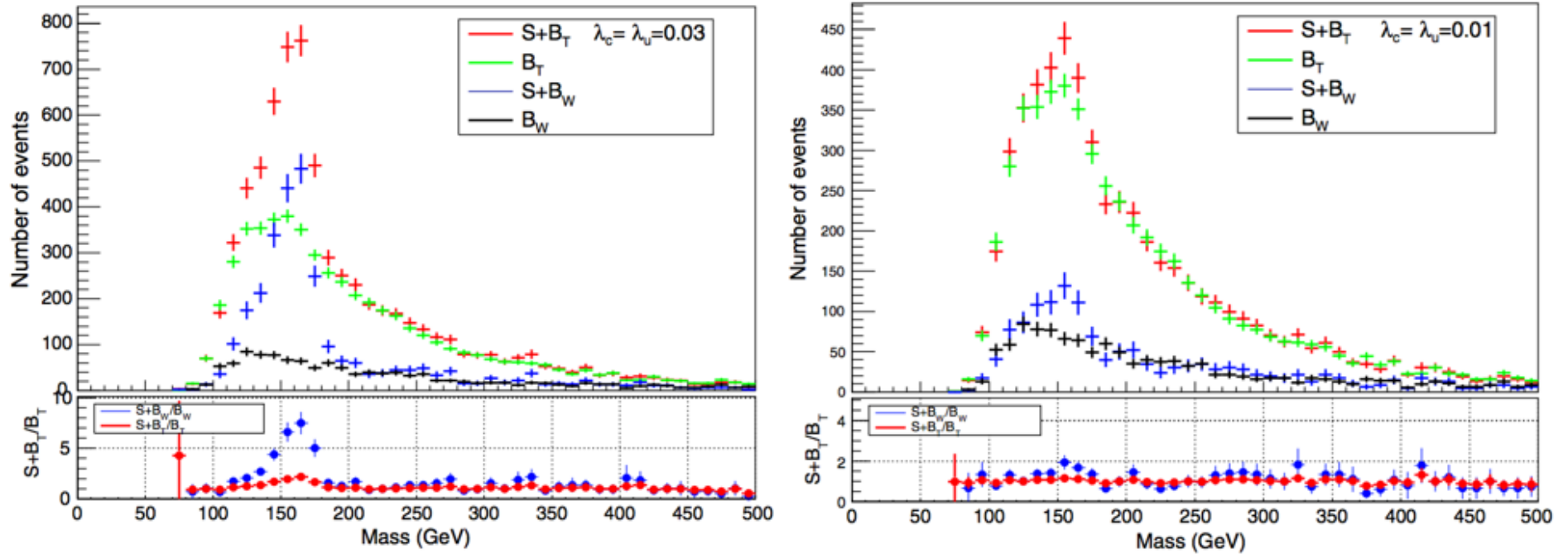
$e^-p \rightarrow e^-Wbq+X$

| FCC-he                | $\lambda_c = 10^{-2}$  | $\lambda_c = 10^{-3}$  | $\lambda_c = 0$        |
|-----------------------|------------------------|------------------------|------------------------|
| $\lambda_u = 10^{-2}$ | $8.106 \times 10^{-3}$ | $5.161 \times 10^{-3}$ | $5.150 \times 10^{-3}$ |
| $\lambda_u = 10^{-3}$ | $3.032 \times 10^{-3}$ | $8.132 \times 10^{-5}$ | $5.142 \times 10^{-5}$ |
| $\lambda_u = 0$       | $2.957 \times 10^{-3}$ | $2.973 \times 10^{-5}$ | 0                      |



## Invariant mass distributions

FCC-eh



Distributions of reconstructed top quark mass plots for signal, and relevant backgrounds, with different anomalous FCNC couplings. The lower part of each plot shows the relative ratio of  $(S+B_T)$  and  $B_T$ . Here, S is for signal and  $B_T$  for total background.



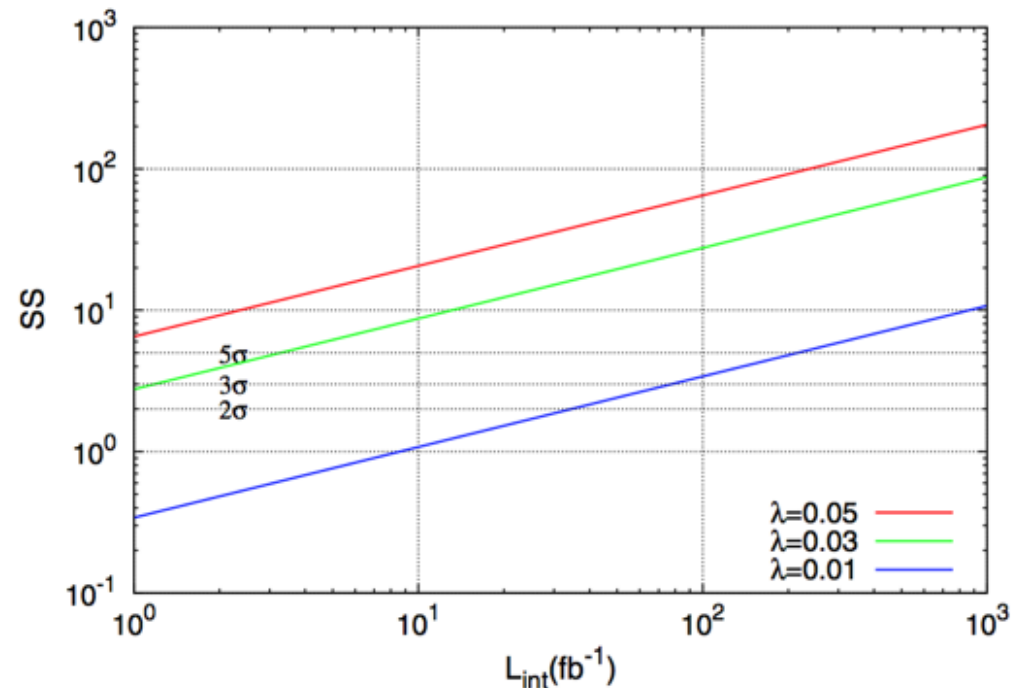
## Number of events and statistical significance

FCC-eh

The number of signal ( $S$ ) and relevant background events ( $B_W$ ,  $B_H$ ,  $B_Z$ ,  $B_{tt}$ ,  $B_{bjj}$ ) after each kinematic cuts in the analysis with  $L_{\text{int}}=100 \text{ fb}^{-1}$  at FCC-eh.

| Processes                      | Cut-0  | Cut-1 | Cut-2 | Cut-3 | Cut-4 | Cut-5 |
|--------------------------------|--------|-------|-------|-------|-------|-------|
| $S + B_W$ ( $\lambda = 0.03$ ) | 206373 | 11687 | 8665  | 7964  | 2867  | 1883  |
| $S + B_W$ ( $\lambda = 0.01$ ) | 200135 | 7827  | 5776  | 5312  | 1396  | 622   |
| $S$ ( $\lambda = 0.03$ )       | 6695   | 4276  | 3218  | 2974  | 1683  | 1440  |
| $S$ ( $\lambda = 0.01$ )       | 457    | 416   | 329   | 322   | 212   | 179   |
| $B_W$                          | 199678 | 7411  | 5447  | 4990  | 1184  | 443   |
| $B_H$                          | 2279   | 979   | 802   | 757   | 107   | 47    |
| $B_Z$                          | 13420  | 1639  | 1145  | 956   | 246   | 110   |
| $B_{tt}$                       | 9752   | 5594  | 5339  | 4974  | 1079  | 460   |
| $B_{bjj}$                      | 48241  | 17287 | 9936  | 9074  | 2573  | 1170  |

On the right (bottom) plot, the statistical significance ( $SS$ ) depending on integrated luminosity for different anomalous FCNC couplings ( $\lambda$ ) are shown for FCC-eh. The  $2\sigma$ ,  $3\sigma$  and  $5\sigma$  lines are also shown.

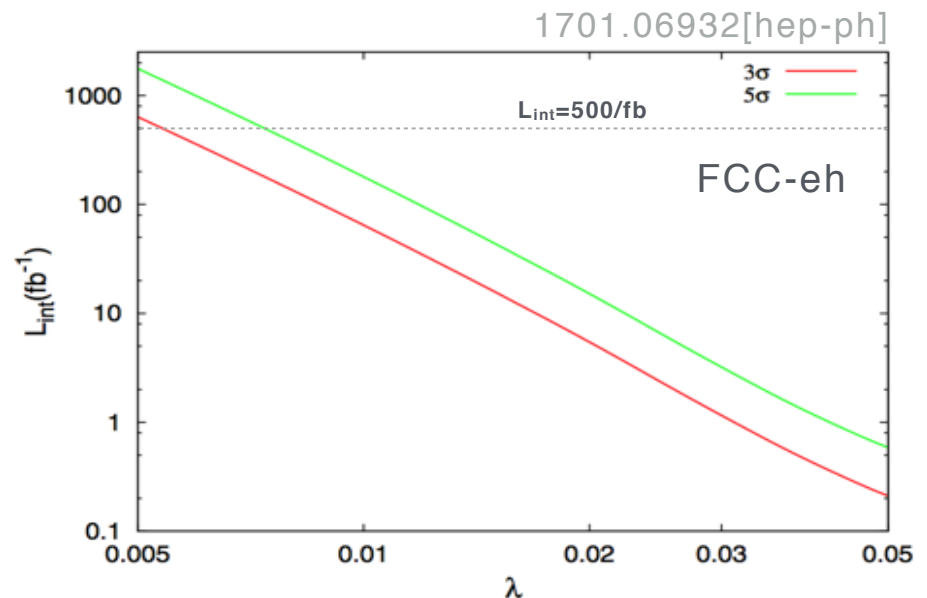
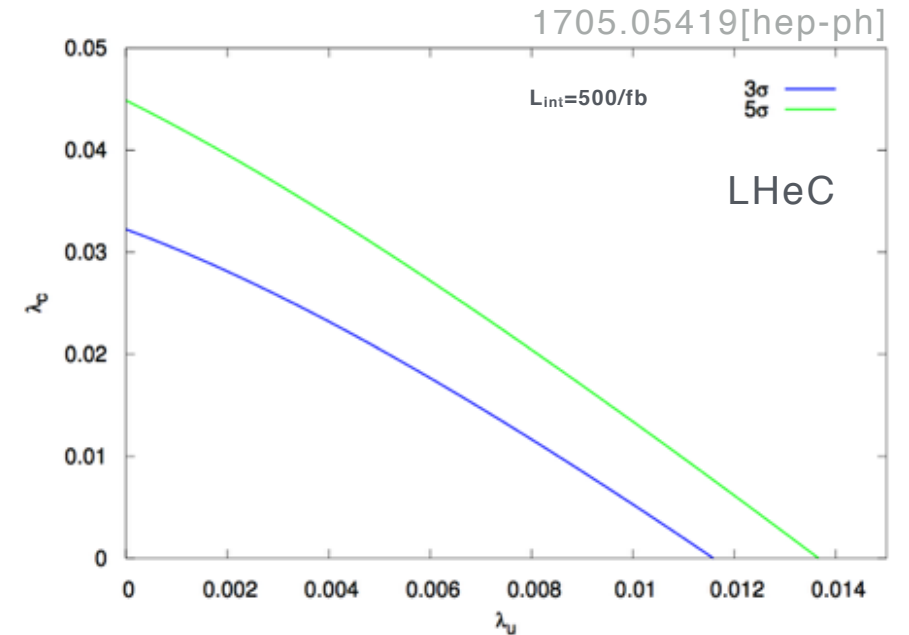


## Results on couplings

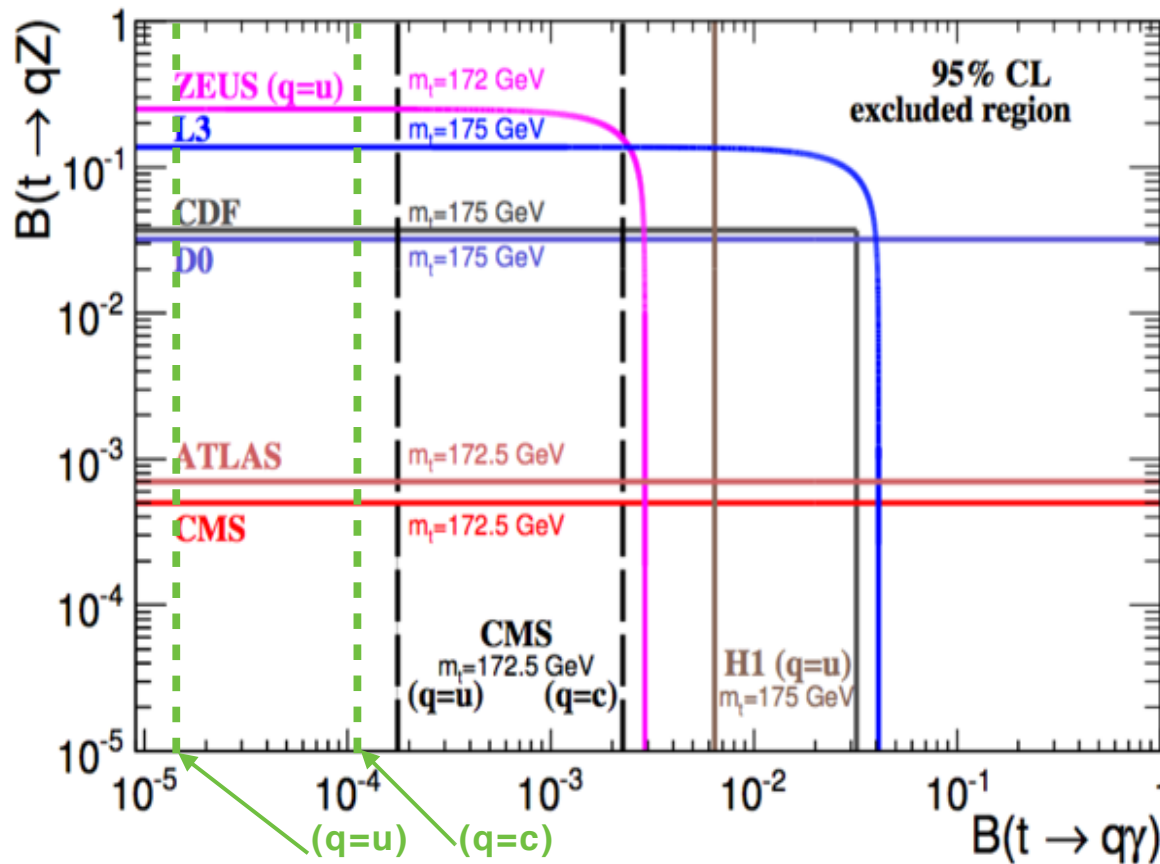
The contour plot for the couplings  $\lambda_u$  and  $\lambda_c$  at LHeC for an integrated luminosity of  $500 \text{ fb}^{-1}$ . The  $3\sigma$  significance results:  $\lambda_u = 0.012$  and  $\lambda_c = 0.032$ . The upper bounds on branching ratios:  $\text{BR}(t \rightarrow u\gamma) < 1.62 \times 10^{-5}$  and  $\text{BR}(t \rightarrow c\gamma) < 1.15 \times 10^{-4}$  at LHeC.

On the right (bottom) plot, the integrated luminosity versus anomalous FCNC coupling ( $\lambda$ ) at  $3\sigma$  and  $5\sigma$  significance is shown for FCC-eh. The results can be compared to the HL-LHC expected limits\*.

\* The expected limits on tq $\gamma$  couplings at HL-LHC have already reported in Ref.[ATLAS Collaboration, arXiv: 1307.7292], the branching ratios for  $t \rightarrow q\gamma$  are  $8 \times 10^{-5}$  and  $2.5 \times 10^{-5}$  for  $L_{\text{int}} = 300 \text{ fb}^{-1}$  and  $3000 \text{ fb}^{-1}$ , respectively.



## Current experimental limits on $tq\gamma$ and $tqZ$



The measured upper limits on  $B(t \rightarrow qZ)$  versus  $B(t \rightarrow q\gamma)$  from different experiments. The two vertical dashed lines show recent results ( $L_{\text{int}}=19.8/\text{fb}$ ) of the analysis of CMS experiment [CMS Collaboration, JHEP04 (2016) 035].

## Conclusion

At the LHeC, we have analyzed the process  $e^-p \rightarrow e^-W^\pm q + X$  with the signature including one isolated electron and one b-jet together with two jets in the final state. The signal for this process includes the top quark flavor changing neutral current couplings ( $tq\gamma$ ) through photon exchanges in electron-proton collisions. We obtain attainable upper limits on the top quark FCNC couplings from the analysis of signal and background including detector effects through the fast simulation.

The FCC-eh, with an electron energy of 60 GeV and a proton energy of 50 TeV, would provide significant single top quark production event rates via investigated channel. Top quark FCNC couplings ( $\lambda > 0.01$ ) can be searched at the level of significance greater than  $3\sigma$  with an integrated luminosity of larger than  $75 \text{ fb}^{-1}$  at the projected FCC-he. The b-tagging has an important role in our study.

The future ep colliders LHeC and FCC-ep with the high luminosity of  $1 \text{ ab}^{-1}$  has the potential in probing the top FCNC couplings ( $\lambda_u, \lambda_c$ ), which can be comparable or even better when compared to the bounds from the HL-LHC.



+

## Current and expected limits on $tq\gamma$ couplings

|                            | LHC<br>(CMS Obs. Limit<br>at 19.8/fb)* | HL-LHC<br>(Expec. Limit<br>at 500/fb)** | LHeC<br>(500/fb)***  | FCC-eh<br>(500/fb)*** |
|----------------------------|--|---|----------------------|-----------------------|
| $B(t \rightarrow u\gamma)$ | $1.3 \times 10^{-4}$                   | $4.5 \times 10^{-5}$                    | $1.6 \times 10^{-5}$ | $6.8 \times 10^{-6}$  |
| $B(t \rightarrow c\gamma)$ | $1.7 \times 10^{-3}$                   | $3.0 \times 10^{-4}$                    | $1.1 \times 10^{-4}$ | $2.4 \times 10^{-5}$  |

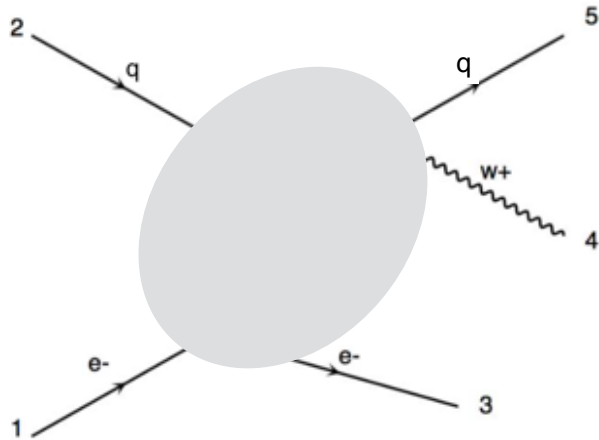
\* Current experimental limit on  $tq\gamma$ , 1511.03951[hep-ex].

\*\* Expected limits for HL-LHC, CMS DP-2016-064.

\*\*\* Current study.

## Cross section

Process:  $e^-p \rightarrow e^-Wq+X$



Cross section (pb) for S+B<sub>W</sub> at LHeC

| $\lambda_u$ or $\lambda_c \rightarrow$ | 0.05  | 0.03  | 0.02  | 0.01  | 0     |
|--|-------|-------|-------|-------|-------|
| $\lambda_c = 0$                        | 2.493 | 2.368 | 2.329 | 2.307 | 2.298 |
| $\lambda_u = 0$                        | 2.324 | 2.308 | 2.303 | 2.299 | 2.298 |
| $\lambda_u = \lambda_c$                | 2.519 | 2.378 | 2.333 | 2.307 | 2.298 |

Cross section (pb) for S+B<sub>W</sub> at FCC-eh

| $\lambda_u$ or $\lambda_c \rightarrow$ | $10^{-1}$ | $10^{-2}$ | $10^{-3}$ |
|--|-----------|-----------|-----------|
| $\lambda(tu\gamma)$                    | 10.72     | 8.58      | 8.57      |
| $\lambda(tc\gamma)$                    | 9.24      | 8.54      | 8.53      |
| $\lambda(tu\gamma,tc\gamma)$           | 11.51     | 8.64      | 8.61      |

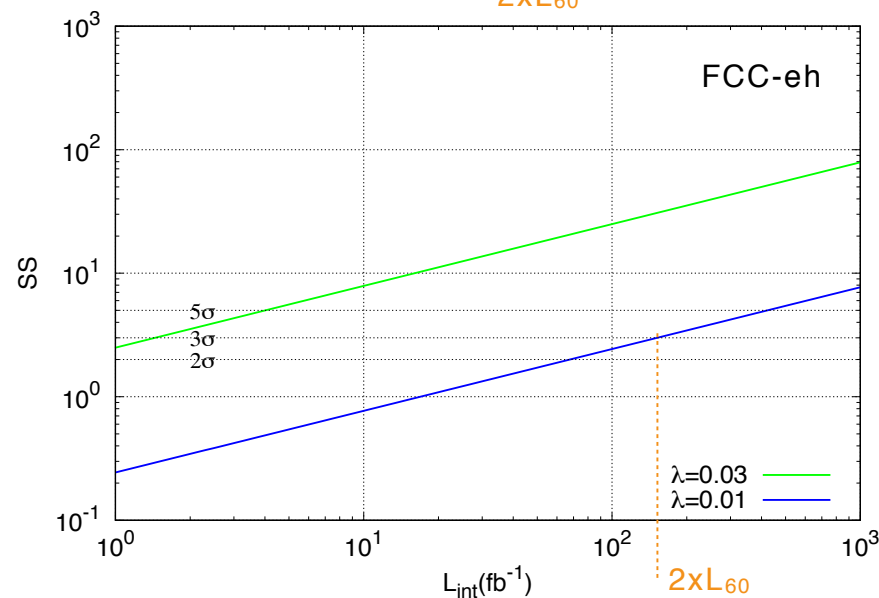
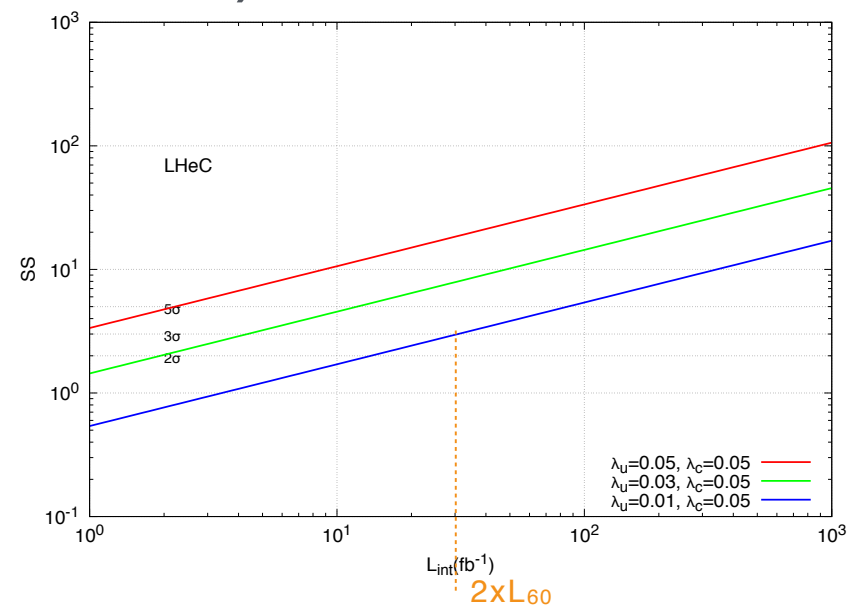
## Comments on lower energy (electron beam) run

- An option with  $E_e=40$  GeV and  $E_p=7$  TeV

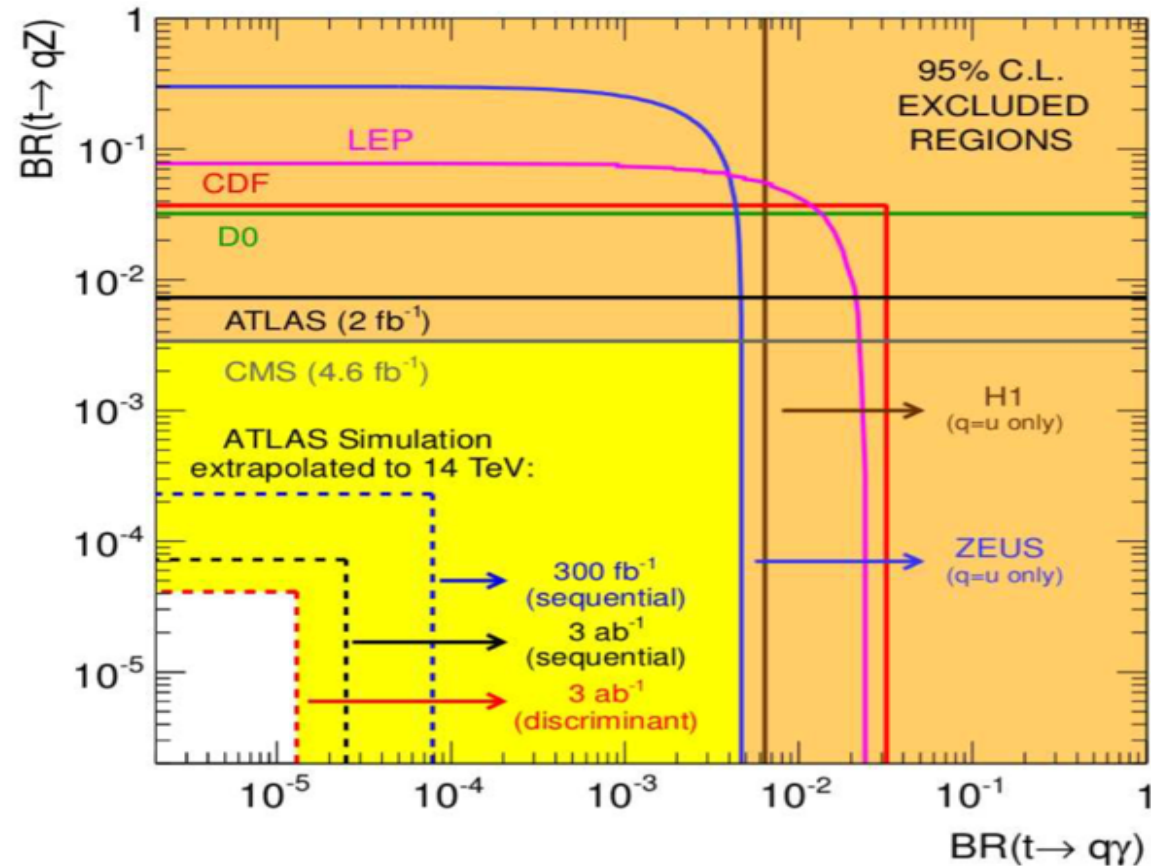
| LHeC      | Cross section (pb) |              |
|-----------|--------------------|--------------|
| $\lambda$ | $E_e=40$ GeV       | $E_e=60$ GeV |
| 0.05      | 1.699              | 2.519        |
| 0.03      | 1.597              | 2.378        |
| 0.01      | 1.546              | 2.307        |

- An option with  $E_e=40$  GeV and  $E_p=50$  TeV

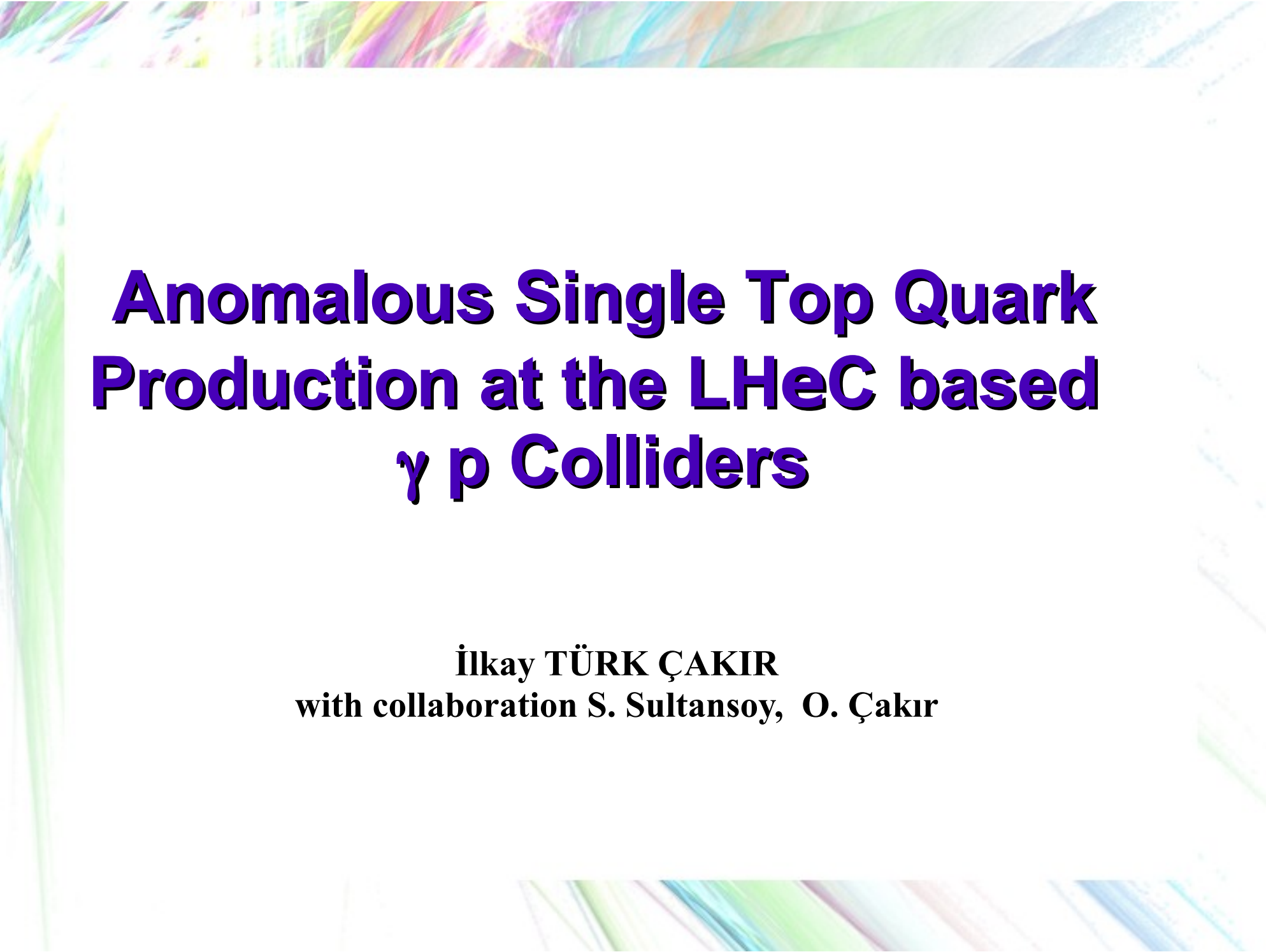
| FCC-eh    | Cross section (pb) |              |
|-----------|--------------------|--------------|
| $\lambda$ | $E_e=40$ GeV       | $E_e=60$ GeV |
| 0.1       | 8.449              | 11.510       |
| 0.03      | 6.451              | 8.932        |
| 0.01      | 6.240              | 8.641        |







The present 95% CL. observed limits on the  $BR(t \rightarrow q\gamma)$  vs.  $BR(t \rightarrow qZ)$  plane are shown as full lines for the LEP, ZEUS, H1, D0, CDF, ATLAS and CMS collaborations. The expected sensitivity at ATLAS is also represented by the dashed lines. For an integrated luminosity of  $L_{int} = 3000 \text{ fb}^{-1}$  the limits range from  $1.3 \times 10^{-5}$  to  $2.5 \times 10^{-5}$  ( $4.1 \times 10^{-5}$  to  $7.2 \times 10^{-5}$ ) for the  $t \rightarrow q\gamma$  ( $t \rightarrow qZ$ ) decay. Limits at  $L_{int} = 300 \text{ fb}^{-1}$  are also shown [ATLAS Collaboration, ATL-PHYS-PUB-2013-007].



# **Anomalous Single Top Quark Production at the LHeC based $\gamma$ p Colliders**

**İlkay TÜRK ÇAKIR**  
with collaboration S. Sultansoy, O. Çakır

# OUTLINE

- Top Quark Properties
- Phenomenology
- FCNC Constraints
  - LEP
  - HERA
  - LHC
- Anomalous top production
- Limits on  $(\kappa_{ut\gamma}, \kappa_{ct\gamma})$
- Conclusion

# Top Quark

The heaviest quark to date, mass  $171.3 \pm 1.2$  GeV

Electric charge  $Q = +2/3$ , and  $T_3 = +1/2$  member of weak isospin

Short life time,  $O(10^{-24} \text{ s})$

Weak decay,  $|V_{tb}| > 0.89$

The ratio  $R = BR(t \rightarrow W^+ b) / BR(t \rightarrow W^+ q) > 0.79$

Top quark could be sensitive to new physics BSM

Anomalous (FCNC) couplings

# Anomalous interactions

Effective lagrangian for the anomalous interaction  $tq\gamma$ ,

$$L = -g_e \sum_{q=u,c} Q_q \frac{\kappa_\gamma^q}{\Lambda} \bar{t} \sigma^{\mu\nu} (f_\gamma^q + h_\gamma^q \gamma_5) q A_{\mu\nu} + h.c.$$

$$A_{\mu\nu} = \partial_\mu A_\nu - \partial_\nu A_\mu$$

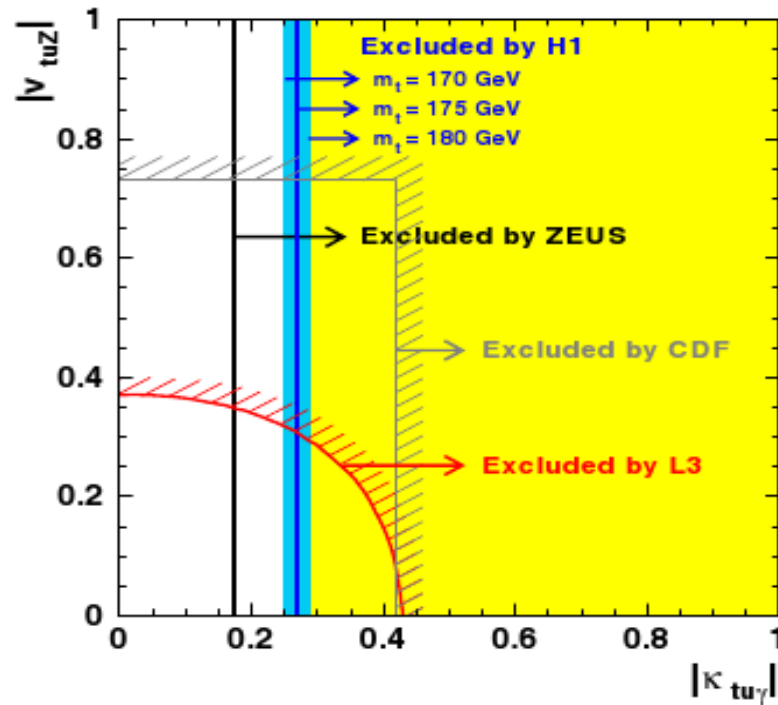
Anomalous decay width ( $t \rightarrow q\gamma$ )

$$\Gamma(t \rightarrow q\gamma) = \left(\frac{\kappa_\gamma^q}{\Lambda}\right)^2 \frac{2}{9} \alpha_{em} m_t^3$$

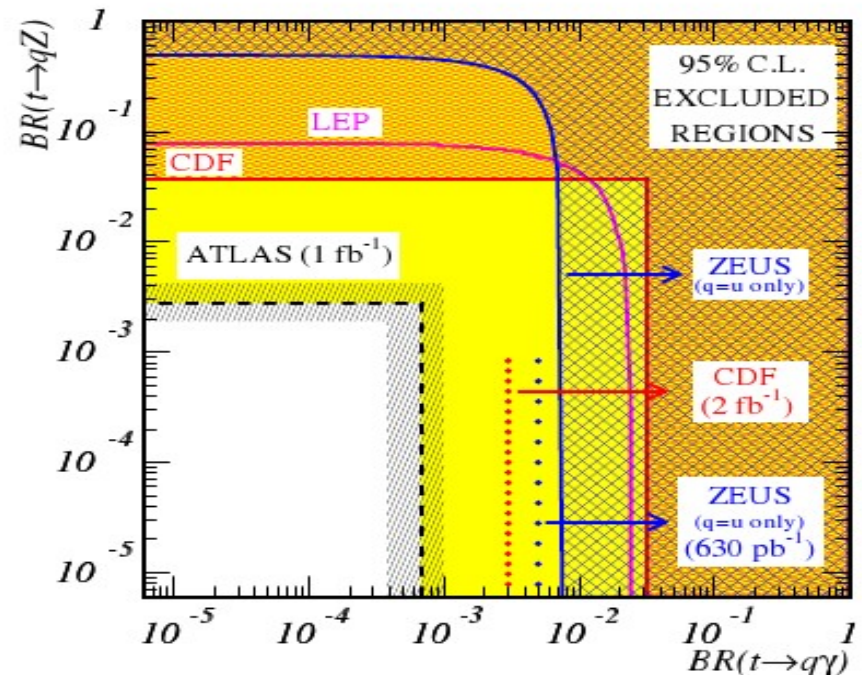


# Top Quark FCNC Constraints from Experiments/Expectations

H1 Collab., EPJC33 (2004)



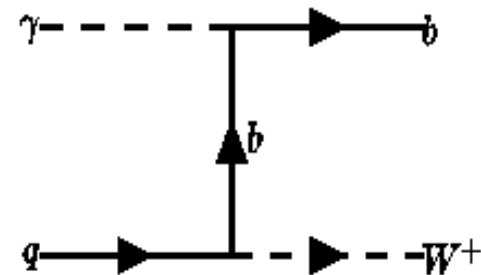
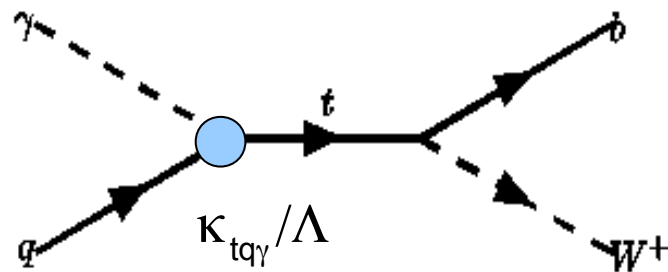
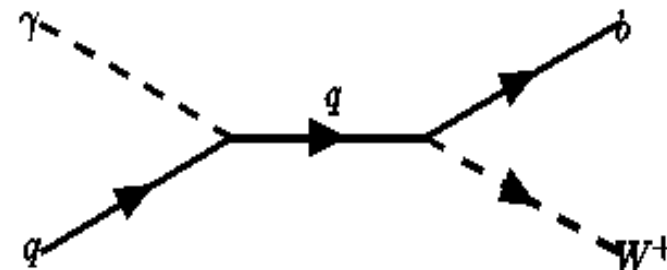
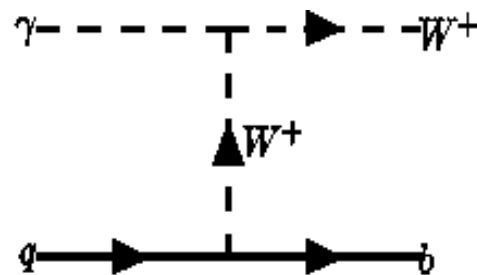
**Constraints on  $\text{Br}(t \rightarrow \gamma q)$**   
 $< 0.0132$  95% CL, [H1 Collab. 2004]  
 $< 0.0059$  95% CL, [ZEUS Collab. 2003]  
 $< 0.041$  95% CL, [L3 Collab. 2002]  
 $< 0.032$  95% CL, [CDF Collab. 1998]



[ATLAS Collab. CERN-OPEN-2008-020]

ATLAS(1fb<sup>-1</sup>) with the conversion  $\kappa_{t\gamma} = 0.059$ .  
 For 100 fb<sup>-1</sup> the expectations  $\kappa_{t\gamma} = 0.01$

# Anomalous production in $\gamma p$ collisions

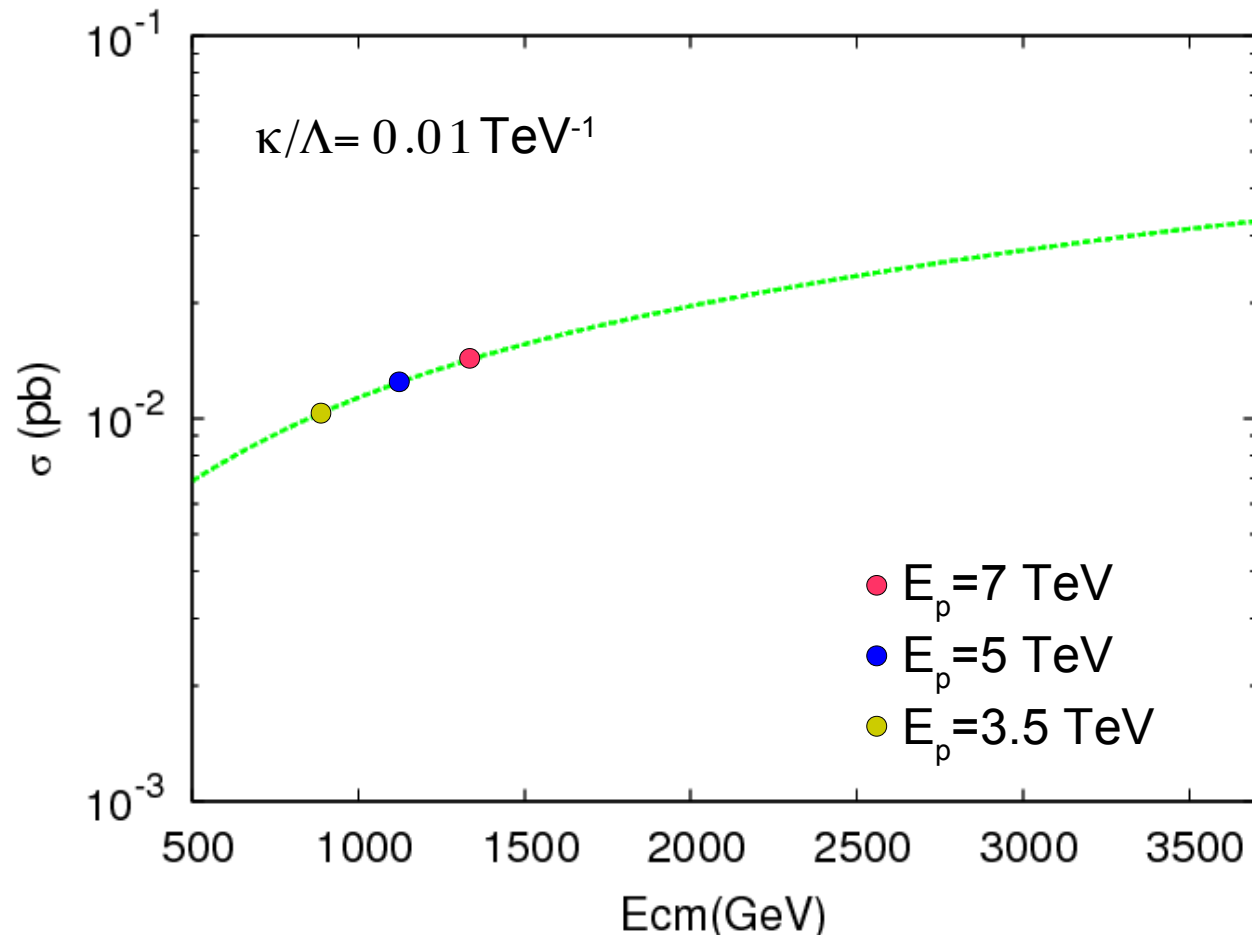


Study the process  $\gamma p \rightarrow W^+ b X$ , and then decay  $W^+ \rightarrow l^+ \nu$

• **Signal:**  $\gamma p \rightarrow t X \rightarrow W^+ b X$

• **Major background:**  $\gamma p \rightarrow (W^+ b, W^+ c, W^+ j) X$ , where  $j = u, d, s$

# Cross section vs center of mass energy ( $E_e=70$ GeV)



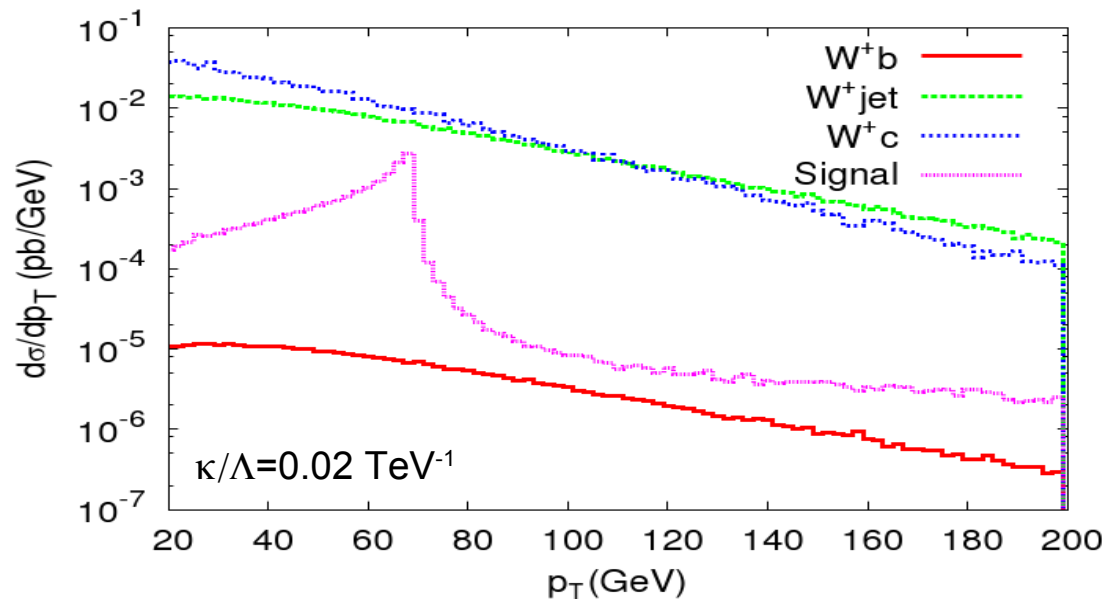
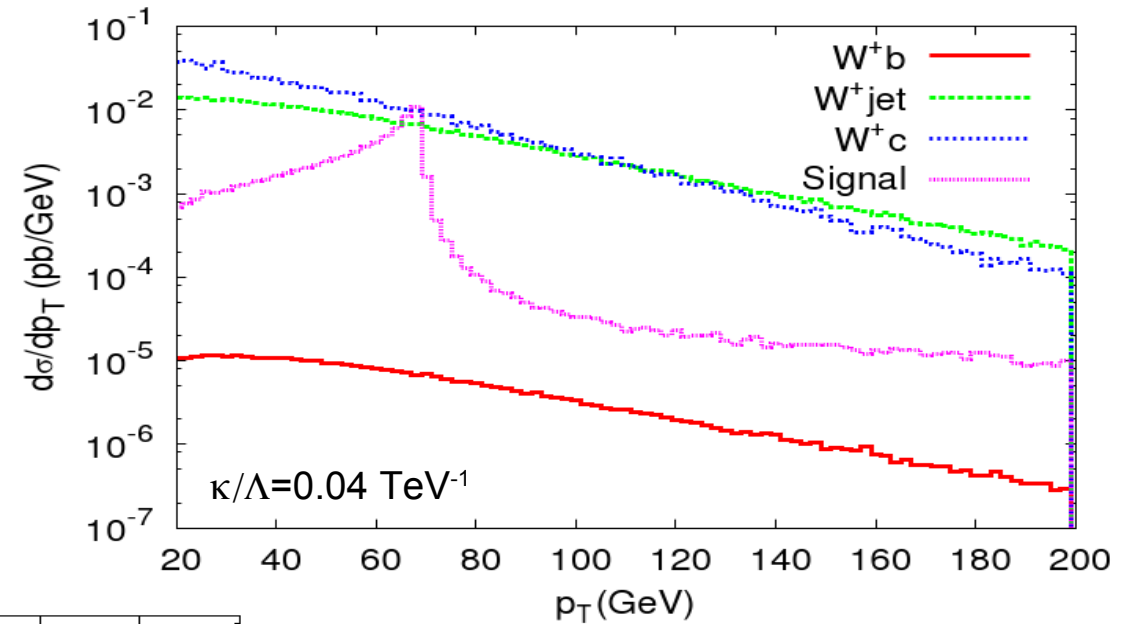


# Cross sections in pb (E:70x7000)

| $\kappa=0.01$  | No cut                 | $p_T > 20$             | $Pt > 40$              | $pt > 50$              |
|----------------|------------------------|------------------------|------------------------|------------------------|
| <b>Signal</b>  | $1.590 \times 10^{-2}$ | $1.527 \times 10^{-2}$ | $1.307 \times 10^{-2}$ | $1.110 \times 10^{-2}$ |
| <b>Bkg: Wb</b> | $1.600 \times 10^{-2}$ | $1.030 \times 10^{-2}$ | $5.800 \times 10^{-3}$ | $4.250 \times 10^{-3}$ |
| <b>Bkg: Wc</b> | $3.106 \times 10^1$    | $1.268 \times 10^1$    | $6.850 \times 10^0$    | $4.900 \times 10^0$    |
| <b>Bkg: Wj</b> | $1.796 \times 10^2$    | $7.237 \times 10^1$    | $4.796 \times 10^1$    | $3.770 \times 10^1$    |

| $\kappa=0.01$  | $M_{Wb}=150-200 \text{ GeV};$<br>$p_T > 20 \text{ GeV}$ | $M_{Wb}=150-200 \text{ GeV};$<br>$p_T > 40 \text{ GeV}$ | $M_{Wb}=150-200 \text{ GeV};$<br>$p_T > 50 \text{ GeV}$ |
|----------------|---|---|---|
| <b>Signal</b>  | $1.476 \times 10^{-2}$                                  | $1.256 \times 10^{-2}$                                  | $1.065 \times 10^{-2}$                                  |
| <b>Bkg: Wb</b> | $2.890 \times 10^{-3}$                                  | $1.869 \times 10^{-3}$                                  | $1.282 \times 10^{-3}$                                  |
| <b>Bkg: Wc</b> | $3.484 \times 10^0$                                     | $2.303 \times 10^0$                                     | $1.635 \times 10^0$                                     |
| <b>Bkg: Wj</b> | $1.393 \times 10^1$                                     | $9.115 \times 10^0$                                     | $6.386 \times 10^0$                                     |

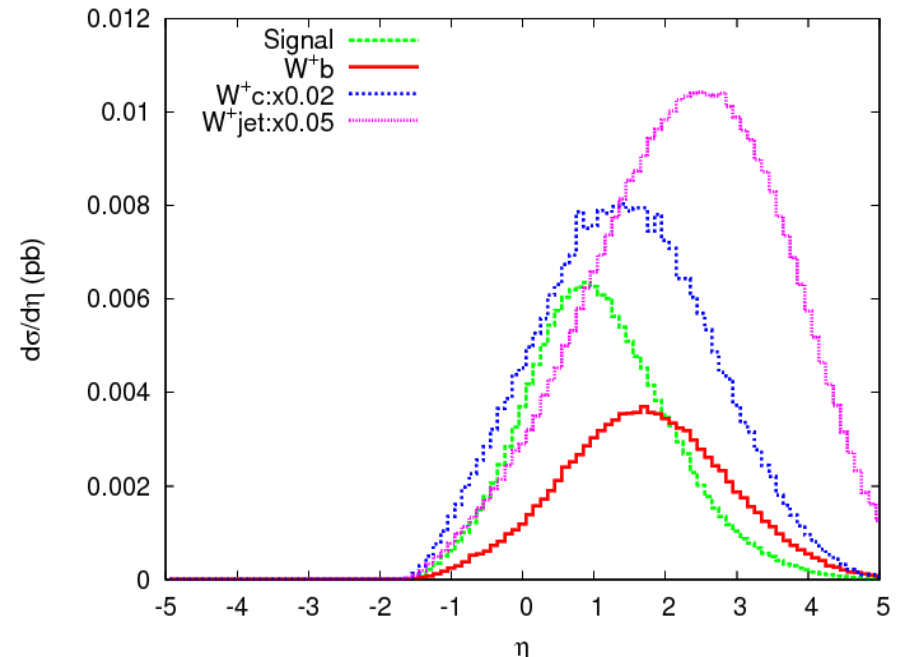
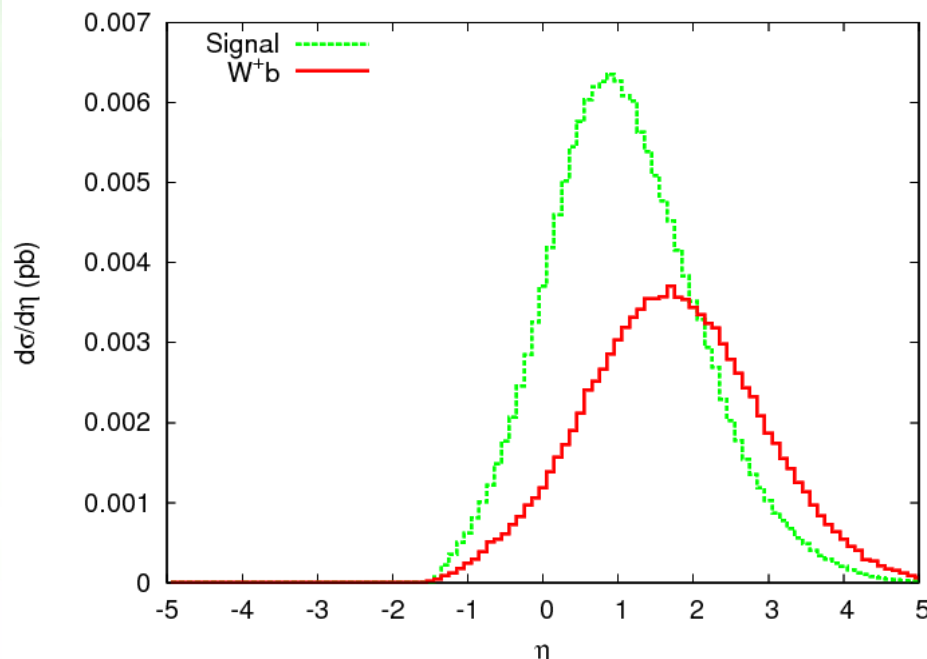
# $p_T$ distribution of b-jet at $\sqrt{s}=1.4$ TeV



where the jets have at least  $p_T > 20$  GeV and the b-tagging is applied with the rejections for light jets <sup>9</sup>

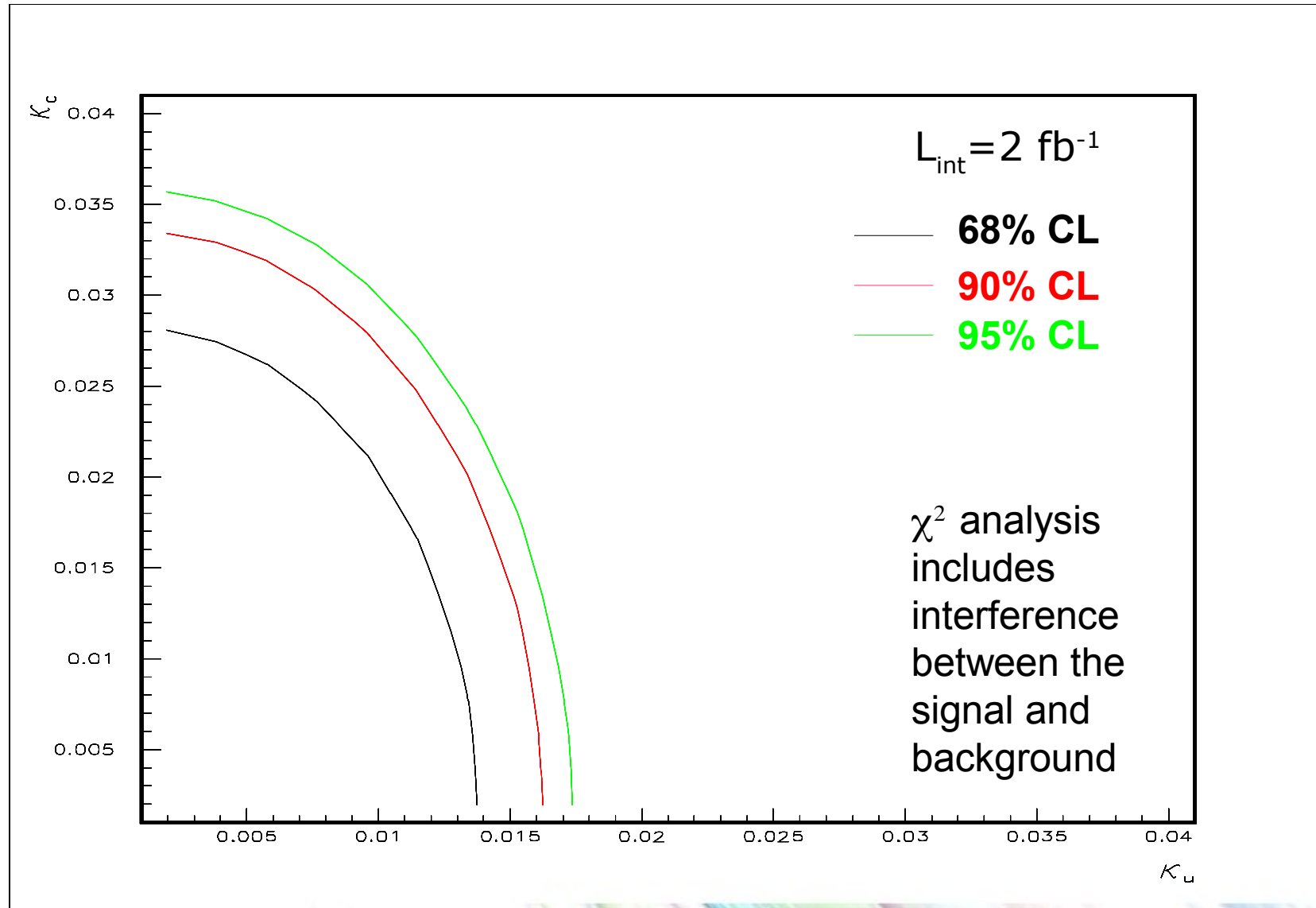
# Rapidity distributions at LHeC(E:70x7000)

Rapidity distribution of b-jets for both signal and corresponding background (IB).

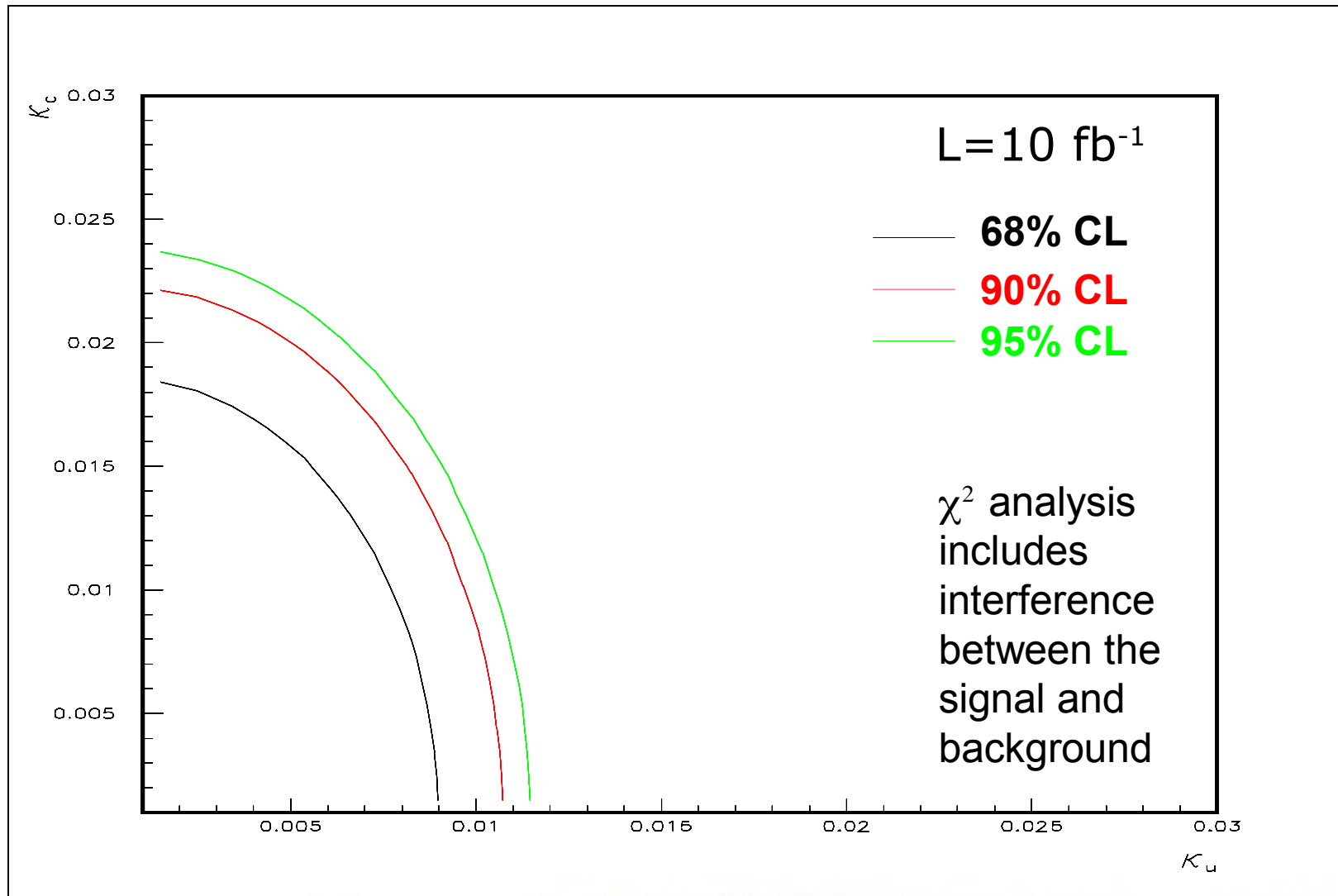


to keep in the same range  $W+c$ (blue) and  $W+j$ (purple) backgrounds (RB) are multiplied with the respective factors.

# Top FCNC discovery at LHeC ( $2 \text{ fb}^{-1}$ )



# Top FCNC discovery at LHeC ( $10 \text{ fb}^{-1}$ )



# Signal Significance

Energy: 70x7000

| cuts   | L=2 fb <sup>-1</sup><br>(κ γ u=0.01)<br>(κ γ c=0.01) | L=10 fb <sup>-1</sup><br>(κ γ u=0.01)<br>(κ γ c=0.01) |
|--|--|---|
| M <sub>wb</sub> =150-200 GeV<br>p <sub>T</sub> =50 GeV | 2.38   | 5.33  |
| M <sub>wb</sub> =150-200 GeV<br>p <sub>T</sub> =40 GeV | 2.58   | 5.79  |

Energy: 140x7000

| cuts   | L=1 fb <sup>-1</sup> (2 fb <sup>-1</sup> )<br>(κ γ u=0.01)<br>(κ γ c=0.01) | L=10 fb <sup>-1</sup><br>(κ γ u=0.01)<br>(κ γ c=0.01) |
|--|--|---|
| M <sub>wb</sub> =150-200 GeV<br>p <sub>T</sub> =50 GeV | 1.88(2.66)   | 5.96  |
| M <sub>wb</sub> =150-200 GeV<br>p <sub>T</sub> =40 GeV | 2.04 (2.88)  | 6.47  |



## CONCLUSION

- Due to its large mass top quark is expected to be sensitive to new physics BSM. In particular, the study of FCNC couplings involving the top quark is well motivated.
- The benefit of b-tagging usage is apparent.
- As precise limits attainable at the LHC, even better limits ( $\kappa_{tu\gamma}/\Lambda=0.01 \text{ TeV}^{-1}$  and  $\kappa_{tc\gamma}/\Lambda=0.02 \text{ TeV}^{-1}$ ) on the anomalous couplings of top quark can be obtained at LHeC based gamma-p collider.